

Published in final edited form as:

J Am Chem Soc. 2002 April 24; 124(16): 4206–4207.

Dipolar Waves as NMR Maps of Protein Structure

Michael F. Mesleh[†], Gianluigi Veglia[‡], Tara M. DeSilva[§], Francesca M. Marassi^{||}, and Stanley J. Opella^{*†}

Department of Chemistry and Biochemistry, University of California, San Diego, La Jolla, California 92093, Department of Chemistry, University of Minnesota, Minneapolis, Minnesota 55485, and The Burnham Institute, 10901 North Torrey Pines Road, La Jolla, California 92037

The anisotropy of nuclear spin interactions results in a unique mapping of structure to the resonance frequencies and splittings observed in NMR spectra. Single crystals provide definitive examples in solid-state NMR spectroscopy¹ However, it is the determination of molecular structure from experimentally measured spectral parameters² that is paramount, and it is this process that is complicated by angular ambiguities resulting from the symmetry properties of dipole–dipole and chemical shift interactions.³ This situation has been substantially improved by the recognition of distinctive wheel-like patterns^{4,5} in two-dimensional ¹H–¹⁵N heteronuclear dipolar/¹⁵N chemical shift PISEMA (polarization inversion spin-exchange at the magic angle) spectra⁶ of helical membrane proteins in highly aligned lipid bilayer samples.⁷ Further, information inherent in anisotropic spectral features can be used to short-circuit the traditional steps of resolution, measurement, and sequential assignment of resonances in protein structure determination.⁸ Weakly aligned samples of proteins display these same effects, primarily as residual dipolar couplings (RDCs), in solution NMR spectra.⁹ This communication introduces one-dimensional dipolar waves as an extension of two-dimensional PISA (polarity index slant angle) wheels to map protein structure in NMR spectra of both highly and weakly aligned samples. It has been well demonstrated that the RDCs aid in the refinement of structures of proteins in solution^{10–12} as well as for the de novo determination of protein folds.^{13–15} In refinement, these measurements supplement an already large number of chemical shifts, approximate distance measurements, and dihedral angle restraints. For the determination of a backbone fold using only RDCs, a large number of measurements (>5 per residue) is a limiting prerequisite.¹⁶ Among the principal advantages of anisotropic spectral parameters in solution NMR spectroscopy is that they report on the global orientations of separate domains of a protein and of individual bonds relative to a reference frame, which reflects the preferred alignment of the molecule in the magnetic field.¹⁷ This does not preclude their utility in characterizing local backbone structure, as has been applied in solid-state NMR of oriented proteins for some time.^{3,18–21}

Spectral simulations indicate that the periodicity inherent in secondary structure elements can be used as an index of their topology.^{4,5} Figure 1A displays classical two-dimensional PISA wheels of an α -helix at four different slant angles relative to the z axis of the oriented molecular frame of reference. Figure 1B illustrates the periodic wavelike variations of the magnitudes of the static heteronuclear dipolar couplings as a function of residue number in the absence of chemical shift effects. At slant angles $>40^\circ$, the absence of information about

© 2002 American Chemical Society

*Author for correspondence. Telephone: (858) 822-4820. Fax: (858) 822-4821. sopella@ucsd.edu.

[†]University of California, San Diego.

[‡]University of Minnesota.

[§]Department of Neurology, Harvard University, Boston, MA 02115.

^{||}The Burnham Institute.

signs of the couplings affects the wave patterns. The corresponding properties of the RDCs in solution NMR spectra of weakly aligned helices for two different rhombicity values are shown in Figure 1, C and D. The striking similarities among the patterns of variation of the dipolar couplings in Figure 1 represent a convergence of solid-state and solution NMR approaches to structure determination.

The observation of the simple recognizable spectral features shown in Figure 1 enables the direct determination of the relative orientations of helices *in a common frame*. When the ^1H - ^{15}N RDCs can be fit to a sinusoid of periodicity ~ 3.6 characteristic of an α -helix, the average value of D_{NH} restricts the possible orientations of the helix to $[\theta_{\text{av}}, \varphi_{\text{av}}]$ as given by

$$D_{\text{NHav}} = D_a \left\{ (3\cos^2\theta_{\text{av}} - 1) + \frac{3}{2}R\sin^2\theta_{\text{av}}\cos 2\varphi_{\text{av}} \right\}$$

where D_a and R are the axial and rhombic components of the alignment tensor of the molecule.²² Because the NH bonds in an α -helix are distributed on a cone with axis θ_{av} , φ_{av} with an aperture angle δ ($=15.8^\circ$), θ oscillates periodically from $\theta_{\text{av}} + \delta$ to $\theta_{\text{av}} - \delta$ and similarly for φ . The sinusoid itself is parametrized as a function of position (x) along the helix ($\rho = 2\pi x/3.6$) by

$$D_{\text{hel}}(\rho) = D_a \left\{ (3\cos^2(\theta_{\text{av}} - \delta\cos\rho) - 1) + \frac{3}{2}R\sin^2(\theta_{\text{av}} - \delta\cos\rho)\cos 2(\varphi_{\text{av}} + \delta\sin\rho) \right\}$$

One sequential or a few residue-type assignments can determine the relative phase of $D_{\text{hel}}(\rho)$, and a fit of the “experimental” sinusoid then yields values for θ_{av} , φ_{av} , D_a , and R . Ambiguities caused by the inherent 4-fold degeneracy of the solutions can be resolved by comparison to a second dataset for a different orientation.²³ The polarity index (rotation) of the helix can be determined from the value of ρ at each residue as well. While similar in some respects to the order matrix analysis for domain orientation, this approach takes advantage of the noncollinearity of the helix axis and the NH bonds in α -helices,^{15,24} Further simplifications result when D_a and R can be estimated by alternative methods. The periodic nature of these patterns lends itself to Fourier analysis.

An experimental dataset of ^1H - ^{15}N RDCs is shown in Figure 2 for MNK1, the first metal-binding domain of the Cu-transporting ATPase involved in Menkes disease.²⁵ The structure shown in Figure 3 was determined in aqueous solution without the use of RDC constraints.²⁵ As shown in Figure 3, the two regions of the protein (residues 18–28 and 61–71) with RDCs that oscillate with a periodicity of 3.6 correspond to the two helices in the protein with an RMSD of 1.8 Hz in both cases. By contrast, the best-fitting sinusoid of periodicity 3.6 for residues 43–53 has an RMSD of 11.3 Hz. The two helices have different average RDCs, and their oscillations have different amplitudes, reflecting differences in the orientations of the helices in the common frame of reference. The orientations of the helices determined from the data in Figure 3, A and B, are shown in Figure 3D, and they are similar to those in the NOE-based protein structure in Figure 3C. The individually fitted values of D_a and R for helices 1 and 2 of 7.91 and 8.37 Hz and 0.56 and 0.59, respectively, are similar to those (8.35 Hz and 0.59) obtained from a global fit of the average structure to the entire NMR dataset with MODULE.²⁶

Dipolar waves are present in many of the experimental RDC datasets archived in BioMagResBank²⁷ and we have found that fits of these data faithfully reproduce the lengths and orientations of the helices in the proteins. A particularly valuable application of dipolar waves is to the determination of the orientations of helices in membrane proteins that are weakly aligned in lipid micelles.^{28,29} Extensions to other types of secondary structure are feasible. Approaches based on orientational constraints lend themselves to high-throughput structure determination because of their effectiveness with limited resonance assignments and the possibility of simultaneously assigning and measuring structural parameters.

Acknowledgments

We thank A. Nevzorov and G. Melacini for many helpful discussions. This research was supported by Grants PO1GM56538, R37GM24266, RO1GM29754, and RO1CA82864 from the National Institutes of Health, and the Biomedical Technology Resource for Solid-State NMR of Proteins supported by Grant P41RR09789.

References

1. Pausak S, Pines A, Waugh JS. *J Chem Phys.* 1973; 59:599–612.
2. Waugh JS. *Proc Natl Acad Sci USA.* 1976; 78:1894–1897.
3. Opella SJ, Stewart PL, Valentine KG. *Q Rev Biophys.* 1987; 19:7–49. [PubMed: 3306759]
4. Marassi FM, Opella SJ. *J Magn Reson.* 2000; 144:150–155. [PubMed: 10783285]
5. Wang J, Denny J, Tian C, Kim S, Mo Y, Kovacs F, Song Z, Nishimura K, Gan Z, Fu R, Quine JR, Cross TA. *J Magn Reson.* 2000; 144:162–167. [PubMed: 10783287]
6. Wu CH, Ramamoorthy A, Opella SJ. *J Magn Reson A.* 1994; 108:270–272.
7. Marassi FM, Ramamoorthy A, Opella SJ. *Proc Natl Acad Sci USA.* 1997; 84:8551–8556. [PubMed: 9238014]
8. Tian F, Valafar H, Prestegard JH. *J Am Chem Soc.* 2001; 123:11791–11796. [PubMed: 11716736]
9. For a review, see: Bax A, Kontaxis G, Tjandra N. *Methods Enzymol.* 2001; 330:127–172. [PubMed: 11462810]
10. Clore GM, Gronenborn AM. *Proc Natl Acad Sci USA.* 1998; 95:5891–5898. [PubMed: 9600889]
11. Tolman JR, Flanagan JM, Kennedy MA, Prestegard JH. *Proc Natl Acad Sci USA.* 1995; 92:9279–9283. [PubMed: 7568117]
12. Mueller GA, Choy WY, Yang D, Forman-Kay JD, Venters RA, Kay LE. *J Mol Biol.* 2000; 300:197–212. [PubMed: 10864509]
13. Hus JC, Marion D, Blackledge M. *J Mol Biol.* 2000; 298:927–936. [PubMed: 10801359]
14. Delaglio F, Kontaxis G, Bax A. *J Am Chem Soc.* 2000; 122:2142–2143. Zweckstetter M, Bax A. *J Am Chem Soc.* 2001; 123:9490–9491. [PubMed: 11562251]
15. Fowler CA, Tian F, Al-Hashimi HM, Prestegard JH. *Mol Biol.* 2000; 304:447–460. Losonszki JA, Andrec M, Fischer MWF, Prestegard JH. *J Magn Reson.* 1999; 138:334–342. [PubMed: 10341140]
16. Hus JC, Marion D, Blackledge M. *J Am Chem Soc.* 2001; 123:1541–1542. [PubMed: 11456746]
17. Skrynnikov NR, Goto NK, Yang D, Choy WY, Tolman JR, Mueller GA, Kay LE. *J Mol Biol.* 1999; 295:1265–1273. [PubMed: 10653702]
18. Cross TA, Opella SJ. *J Mol Biol.* 1985; 182:367–381. [PubMed: 4009711]
19. Ketchum RR, Hu W, Cross TA. *Science.* 1993; 261:1457–1460. [PubMed: 7690158]
20. Opella SJ, Marassi FM, Gesell JJ, Valente AP, Kim Y, Oblatt-Montal M, Montal M. *Nat Struct Biol.* 1999; 6:374–379. [PubMed: 10201407]
21. Wang J, Kim S, Kovacs F, Cross TA. *Protein Sci.* 2001; 10:2241. [PubMed: 11604531]
22. Clore GM, Gronenborn AM, Tjandra N. *J Magn Res.* 1998; 131:159–162.
23. Al-Hashimi HM, Valafar H, Terrell M, Zartler ER, Eidness MK, Prestegard JH. *J Magn Reson.* 2000; 143:402–406. [PubMed: 10729267]

24. Fischer MWF, Losonsczi JA, Weaver JL, Prestegard JH. *Biochemistry*. 1999; 38:9013–9022. [PubMed: 10413474]
25. PDB structure 1KVI.
26. Dosset P, Hus JC, Marion D, Blackledge M. *J Biomol NMR*. 2001; 20:223–231. [PubMed: 11519746]
27. <http://www.bmrb.wisc.edu/>.
28. Ma C, Opella SJ. *J Magn Reson*. 2000; 146:381–384. [PubMed: 11001856] Veglia G, Opella SJ. *J Am Chem Soc*. 2000; 122:11733–11734.
29. Chou JJ, Kaufman JD, Stahl SJ, Wingfield PT, Bax A. *J Am Chem Soc*. 2002; 124:2450–2451. [PubMed: 11890789]

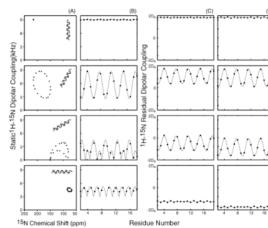


Figure 1. Simulated ^1H - ^{15}N heteronuclear dipolar couplings for an 18-residue ideal ($\Phi = -65^\circ$, $\Psi = -40^\circ$) α -helix for slant angles of 0° , 30° , 60° , and 90° . (A) PISA wheels for a fully aligned protein showing the dipolar couplings as a function of ^{15}N chemical shift. (B) dipolar waves showing the static dipolar couplings of the PISA wheels as a function of residue position. (C and D) dipolar waves showing the residual dipolar couplings of a weakly aligned protein as a function of residue position in helices with average slant angles in the oriented frame C. Rhombicity of 0.25 D. Rhombicity of 0.6. The magnitude of the alignment D_a contributes to scaling of the values in C and D.

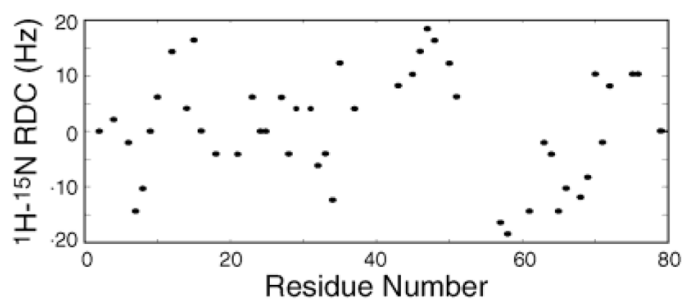


Figure 2. Experimental ^1H - ^{15}N residual dipolar couplings for the 79-residue protein MNK1. RDCs were measured by comparing ^1H - ^{15}N couplings measured in isotropic solution and in the presence of magnetically aligned Pf1 bacteriophage.

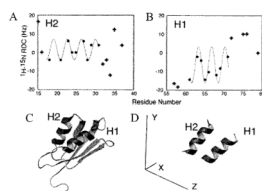


Figure 3.

Experimental ^1H - ^{15}N residual dipolar couplings for the (A) first helix and (B) second helix of MNK1 show the best-fitting sinusoid. The average solution NMR structure (C) is shown in the oriented frame compared to (D) orientations of the two helices obtained by the fitting algorithm. The average solution NMR structure (C) is shown in the oriented frame compared to (D) orientations of the two helices obtained by the fitting algorithm.